ORIGINAL ARTICLE

Adipose Tissue Dysfunction Signals Progression of Hepatic Steatosis Towards Nonalcoholic Steatohepatitis in C57Bl/6 Mice

Caroline Duval,[1,2] Uwe Thissen,[2,3] Shohreh Keshtkar,[1,2] Bertrand Accart,[1,2] Rinke Stienstra,[1,2] Mark V. Boekschoten,[1,2] Tania Roskams,[4] Sander Kersten,[1,2] and Michael Müller[1,2]

OBJECTIVE—Nonalcoholic fatty liver disease (NAFLD) is linked to obesity and diabetes, suggesting an important role of adipose tissue in the pathogenesis of NAFLD. Here, we aimed to investigate the interaction between adipose tissue and liver in NAFLD and identify potential early plasma markers that predict nonalcoholic steatohepatitis (NASH).

RESEARCH DESIGN AND METHODS—C57Bl/6 mice were chronically fed a high-fat diet to induce NAFLD and compared with mice fed a low-fat diet. Extensive histological and phenotypical analyses coupled with a time course study of plasma proteins using multiplex assay were performed.

RESULTS—Mice exhibited pronounced heterogeneity in liver histological scoring, leading to classification into four subgroups: low-fat low (LFL) responders displaying normal liver morphology, low-fat high (LFH) responders showing benign hepatic steatosis, high-fat low (HFL) responders displaying pre-NASH with macrovesicular lipid droplets, and high fat high (HFH) responders exhibiting overt NASH characterized by ballooning of hepatocytes, presence of Mallory bodies, and activated inflammatory cells. Compared with HFL responders, HFH mice gained weight more rapidly and exhibited adipose tissue dysfunction characterized by decreased final fat mass, enhanced macrophage infiltration and inflammation, and adipose tissue remodeling. Plasma haptoglobin, IL-1β, TIMP-1, adiponectin, and leptin were significantly changed in HFH mice. Multivariate analysis indicated that in addition to leptin, plasma CRP, haptoglobin, eotaxin, and MIP-1α early in the intervention were positively associated with liver triglycerides. Intermediate prognostic markers of liver triglycerides included IL-18, IL-1β, MIP-1γ, and MIP-2, whereas insulin, TIMP-1, granulocyte chemotactic protein 2, and myeloperoxidase emerged as late markers.

CONCLUSIONS—Our data support the existence of a tight relationship between adipose tissue dysfunction and NASH pathogenesis and point to several novel potential predictive biomarkers for NASH. *Diabetes* 59:3181–3191, 2010

Obesity is associated with a number of metabolic perturbations that increase risk for type 2 diabetes, coronary heart disease, and liver dysfunction. These metabolic perturbations, collectively referred to as the metabolic syndrome, include hypertension, dyslipidemia, and insulin resistance. Additionally, metabolic syndrome is often characterized by nonalcoholic fatty liver disease (NAFLD) (1).

It is evident that obesity represents a state of chronic low-grade inflammation that likely originates in the adipose tissue. Upon fat expansion, macrophages and other leukocytes infiltrate the adipose tissue and account for secretion of various cytokines and adipokines (2,3). Because many of these cytokines reduce insulin sensitivity, the elevated inflammatory status may provide a mechanistic explanation for the well-established link between obesity and insulin resistance (4). Alternatively, the complications of obesity may be traced to aberrant storage of lipids in nonadipose tissues, which can profoundly disturb organ function (5).

Excess storage of fat in liver is the hallmark of NAFLD, which refers to a wide histological spectrum of liver diseases ranging from hepatic steatosis to pathological nonalcoholic steatohepatitis (NASH) and fibrotic complications (6). Steatosis alone is considered relatively innocuous, but prognosis is much more grim for NASH, which might progress to cirrhosis and liver cancer (7). Several theories have been proposed to explain why steatosis occasionally progresses to NASH. One popular model is the two-hit hypothesis, in which the first hit is the accumulation of fat in the hepatocytes that renders the liver more susceptible to second hits comprised of inflammatory insults or oxidative stress (7). Alternatively, progression of steatosis to NASH may be stimulated by cellular lipotoxicity mediated by lipotoxic fatty acids, cholesterol, and/or ceramides (8).

Since NAFLD is strongly linked to obesity, an important role of adipose tissue in the pathogenesis of NAFLD is suspected. Indeed, growing evidence indicates that proteins secreted from adipose tissue may be implicated in NAFLD (9). To gain insight into the nature of the interaction between adipose tissue and liver in the context of obesity-related NAFLD and to identify potential early plasma markers that predict steatosis and/or NASH, we subjected C57Bl/6 mice to a chronic high-fat diet to induce NAFLD and coupled extensive histological and phenotypical analyses with a time course study of plasma proteins using multiplex assay. The results indicate a tight relationship between adipose tissue dysfunction and NASH patho-

genesis and point to several novel potential predictive biomarkers for NASH.

RESEARCH DESIGN AND METHODS

Twenty male C57BL/6JOlaHsd (C57Bl/6) mice at 8 weeks of age were purchased from Harlan (Horst, the Netherlands) and housed individually. Detailed information about the mouse strain is available at the following Web site: http://www.harlan.com/research_models_and_services/research_models_by_product_type/inbred_mice/c57bl6j_inbred_mice.hl. After 3 weeks on a low-fat diet (LFD), mice were divided into two weight-matched groups. One group continued on the LFD while the other group switched to a high fat diet (HFD) containing 10 or 45% energy as triglycerides, respectively (D12450B and D12451; Research Diets) for 21 weeks. Lard in these diets was replaced by palm oil. Palm oil is devoid of cholesterol, which may have proinflammatory properties. Food intake was measured by weighing the pellets once per week. Mice were housed individually, allowing for assessment of food consumption of individual mice. Food intake was averaged over the 20-week intervention and multiplied by the caloric value of the feed to determine energy intake in kcal · mouse^{-1} · day^{-1}. Numbers were subsequently averaged per group. At weeks 0, 2, 4, 8, 12, 16, and 20, tail vein plasma samples were collected after a 6-h fast. Two mice within the HFD group died before the end of the experiment for reasons unrelated to the dietary intervention. After 21 weeks, ad libitum–fed mice were anesthetized using isofluorane. Blood was collected by orbital puncture, followed by sacrifice via cervical dislocation. Liver and epididymal white adipose tissues were removed, weighed, and immediately frozen in liquid nitrogen. For histology, liver was frozen with OCT compound, and adipose tissue samples were fixed in 10% formalin and processed for paraffin embedding. Animal experiments were approved by the local animal ethics committee at Wageningen University.

Hepatic triglyceride content determination, RNA extraction, real-time PCR, and Affymetrix Microarrays. Liver triglycerides were determined enzymatically as previously described (10). Other techniques were employed as previously described (11). Microarray data were analyzed as previously described (12). Genes with a P value <0.05 were considered significantly regulated. Array data have been submitted to the Gene Expression Omnibus (accession no. GSE24031). Gene set enrichment analysis was used to identify significantly regulated pathways (13). Gene sets with a false discovery rate <0.25 were considered significant.

Plasma measurements. Plasma concentrations of multiple chemokines were measured with multiplex technologies (Rodent Map 2.0; Rules Based Medicine, Austin, TX). Plasma free fatty acids and alanine aminotransferase were measured with commercially available kits from Instruchemie (Delfzijl, the Netherlands). Plasma leptin and insulin levels were measured using kits from Linco (St. Louis, MO).

Liver immunohistochemistry. For oil red O staining, 5 μm frozen liver sections were air-dried for 30 min, followed by fixation in formal calcium (4% formaldehyde and 1% CaCl$_2$). Oil red O staining was performed using standard protocols. Hematoxylin-eosin (H-E) staining of frozen liver sections was carried out as described at http://www.ihcworld.com/histology.htm. Collagen was stained using fast green FCF/sirius red F3B.

For immunohistochemistry, 5 μm frozen liver sections were cut, dried overnight, fixed in acetone for 10 min, and washed in PBS prior to use. For visualization of hepatic stellate cell activation, rabbit anti–glial fibrillary acidic protein (GFAP) polyclonal antibody was used (Dako, Glostrup, Denmark). For detection of macrophages/monocytes, a rat polyclonal anti-Cd68 antibody (Serotec, Oxford, U.K.) was used. Sections were incubated for 30 min at room temperature with GFAP (1:1,000 dilution) or Cd68 (1:100 dilution) primary antibodies, followed by incubation for 30 min at room temperature with anti-rabbit peroxidase-conjugated En Vision (GFAP; Dako) or 1:20 diluted anti-rat IgG peroxidase-conjugated secondary antibodies (Cd68; Serotec). Visualization of the complex was done using 3-amino-9-ethylcarbazole chromogen for 15 min, followed by staining with H-E. Negative controls were performed by omitting the primary antibody.

Immunohistochemistry of adipose tissue. 5-μm-thick paraffin-embedded sections were cut, dried for 30 min at 37°C, and washed in PBS prior to use. Staining of adipose tissue macrophages was carried out using an antibody against Cd68 as described above. H-E staining of sections was done using standard protocols. Collagen was stained using fast green FCF/sirius red F3B.

Multivariate Rules-Based Medicine data analysis. The data obtained from the commercial Rules-Based Medicine multiplex analysis (70 proteins measured in 126 plasma samples) contained a number of technically unreliable entries for specific samples and proteins that were: 1) lower than the least detectable dose (LDD): replaced by 0.5 × LDD, 2) not detectable (i.e., not measured on the standard curve): replaced by 0.1 × LDD, or 3) not measurable (i.e., not sufficient sample material available): replaced by 0.1 × LDD. Proteins were removed if they did not contain more than 50% reliable entries for two or more groups of the totally available 14 groups (7 time points × 2 diets). This approach assures that potentially relevant group differences are retained in the data. Of the 70 proteins screened, 19 were excluded, 18 contained more than 50% reliable entries for at least two groups, and 33 proteins contained 100% reliable entries for all groups. One mouse was removed from the dataset for multivariate analysis on the basis that some plasma proteins display atypical outlying values.

Multiway partial least squares (PLS) (MPLS) is a multivariate statistical technique that is an extension of standard PLS analysis able to analyze data across different time points (14–16). Both methods are able to analyze large numbers of variables in small sample sizes by reducing the dimensionality of the data. In contrast to standard two-dimensional data (matrix), multiway data can be represented as a collection of matrices (a cube) where each matrix contains data from one specific time point. For MPLS, the data were centered across the samples (i.e., zero mean) to remove offsets followed by autoscaling for the variables (i.e., a mean ± SD of 0 ± 1 to remove arbitrary differences in measurement scales [16]).

Validation of the MPLS models using a double cross-validation strategy and the selection of most important proteins from the models have been performed as previously described (17). Because (double) cross-validation relies on a random subdivision of data, the complete validation procedure was repeated five times on the basis of different random subdivisions of the data during cross-validation. A model was considered to be reliable if at least four (out of five) models could be calculated with an $R^2 > 0.7$.

Statistical analyses. Statistically significant differences were calculated using Student's T test. The cutoff for statistical significance was set at $P < 0.05$. MPLS was performed using the N-way toolbox (http://www.models.life.ku.dk/nwaytoolbox) in combination with Matlab, version 7.1.0, release 14 (The Mathworks, Natick, MA) and homemade software.

RESULTS

Development of NASH in a subpopulation of C57Bl/6 mice fed a HFD. To study the effect of chronic high-fat feeding on liver metabolic functions, C57Bl/6 mice were fed an LFD or HFD for 21 weeks. Mice fed the HFD gained more weight compared with mice fed the LFD (Fig. 1A), which was already evident after 2 weeks. Enhanced weight gain in mice fed a HFD may be related to increased energy intake (Fig. 1B). After 21 weeks, weight of the epididymal fat pad, which was assumed to reflect overall adiposity of the animals, was markedly higher in mice fed an HFD (Fig. 1C).

To characterize the effect of an HFD on hepatic steatosis, liver sections were stained with H-E (Fig. 1D) and oil red O (Fig. 1E). Remarkably, a marked heterogeneity in fat accumulation and histology was observed within each group. Scoring of the sections by a pathologist (T.R.) indicated different stages of NAFLD and led to classification of mice into four subgroups, which surprisingly but not deliberately ended up being of approximately equal size. These subgroups were low-fat low (LFL) responders (n = 4), which display normal liver morphology; low-fat high (LFH) responders (n = 6), which develop benign hepatic steatosis; high-fat low (HFL) responders (n = 4), which show a pre-NASH phenotype of macrovesicular lipid droplets; and high-fat high (HFH) responders (n = 4), which develop overt NASH characterized by ballooning of hepatocytes, presence of Mallory bodies, and activated inflammatory cells (Fig. 1D).

Quantitation of hepatic triglycerides confirmed the heterogeneity between the subgroups, with HFH mice accumulating the highest amount of triglycerides (Fig. 1F). Consequently, liver–to–body weight ratio was increased specifically in HFH mice, indicating hepatomegaly (Fig. 1G). Finally, plasma alanine aminotransferase activity was highest in the HFH subgroup, reflecting increased liver damage (Fig. 1H).
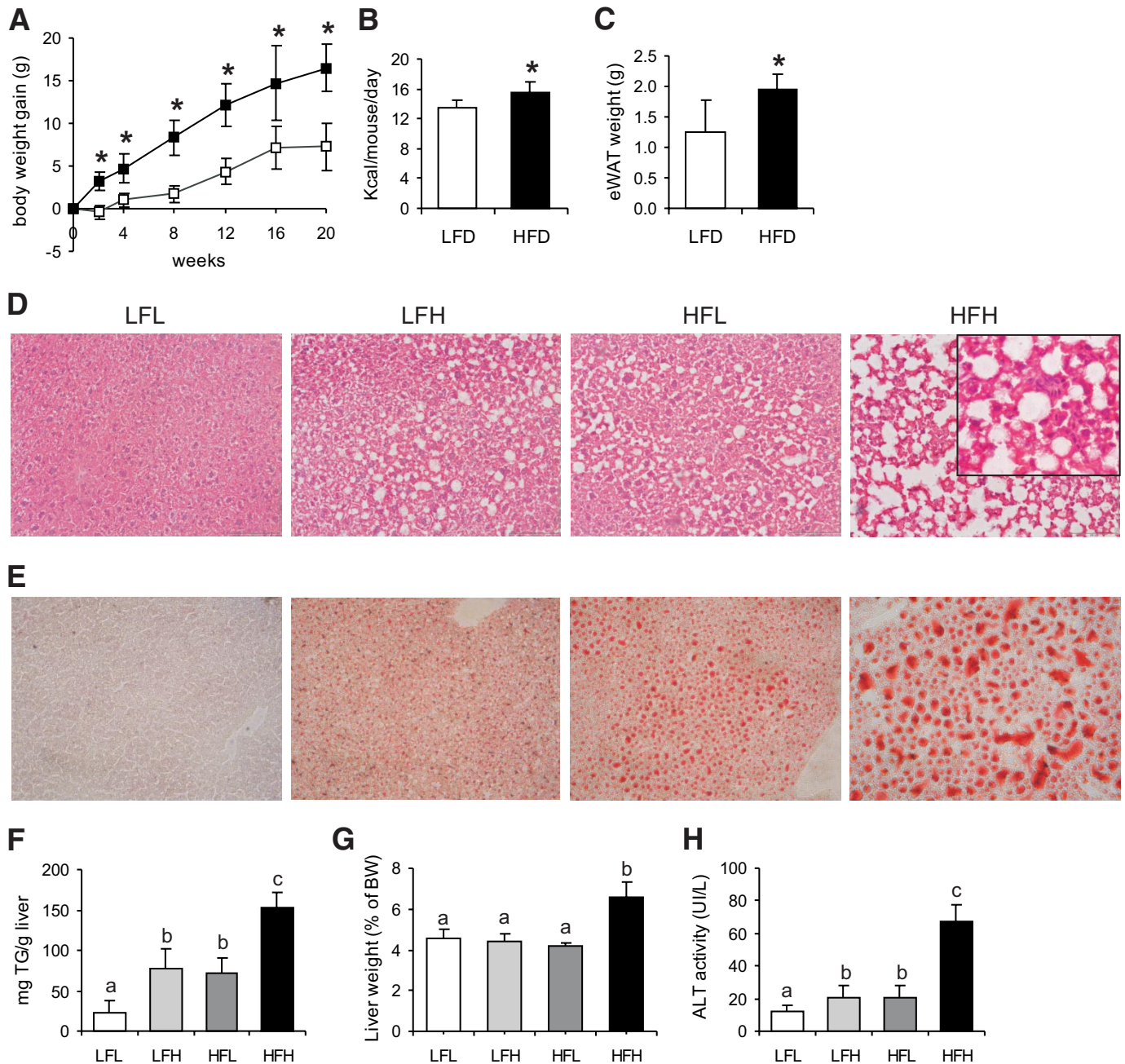
FIG. 1. A subpopulation of mice fed an HFD develops NASH. *A*: Changes in body weight in C57Bl/6 mice fed an LFD (□; n = 10) or HFD (■; n = 8). *B*: Mean energy intake of mice fed an LFD or HFD during 21 weeks of dietary intervention. *C*: Weight of epididymal fat pad after 21 weeks of dietary intervention. Error bars reflect SD. *Significantly different from mice fed an LFD according to Student's *t* test (P < 0.05). H-E staining (*D*) and oil red O staining (*E*) of representative liver sections of the four subgroups (LFL, LFH, HFL, and HFH). *F*: liver triglyceride concentration. *G*: Liver weight (expressed as percentage of total body weight [BW]). *H*: Activity of alanine aminotransferase (ALT) (glutamate pyruvate transaminase) in plasma. Error bars reflect SD. Bars with different letters are statistically different (P < 0.05 according to Student's *t* test). n = 4 mice per group for LFL, HFL, and HFH, and n = 6 mice per group for LFH. (A high-quality digital representation of this figure is available in the online issue.)

NASH-related metabolic pathways are exclusively impaired in HFH Responders. To correlate changes in liver functions with gene expression, expression profiling was performed on individual mouse livers. Microarray data were processed according to subgroups, with LFL mice serving as the reference group for calculation of fold change and *P* values. The most dramatic effects were observed in HFH responders as shown by changes in expression of >3,000 genes (Fig. 2*A*). To identify genes regulated exclusively in HFH responders, we selected genes that were statistically significantly regu-

lated in HFH versus all subgroups but unchanged in other comparisons. This HFH responder gene expression signature comprised 388 upregulated and 319 downregulated genes. One dominant pathway within the HFH expression signature was lipid metabolism, illustrated by the marked induction of *Cidec* and *Mogat1* (Fig. 2*B*). Other lipid metabolism genes such as *Cd36* and *Pparγ* increased gradually from LFL to HFH, correlating with hepatic triglycerides (Fig. 1*F* and Fig. 2*B*). Another pathway well represented within the HFH expression signature was inflammation, as shown by
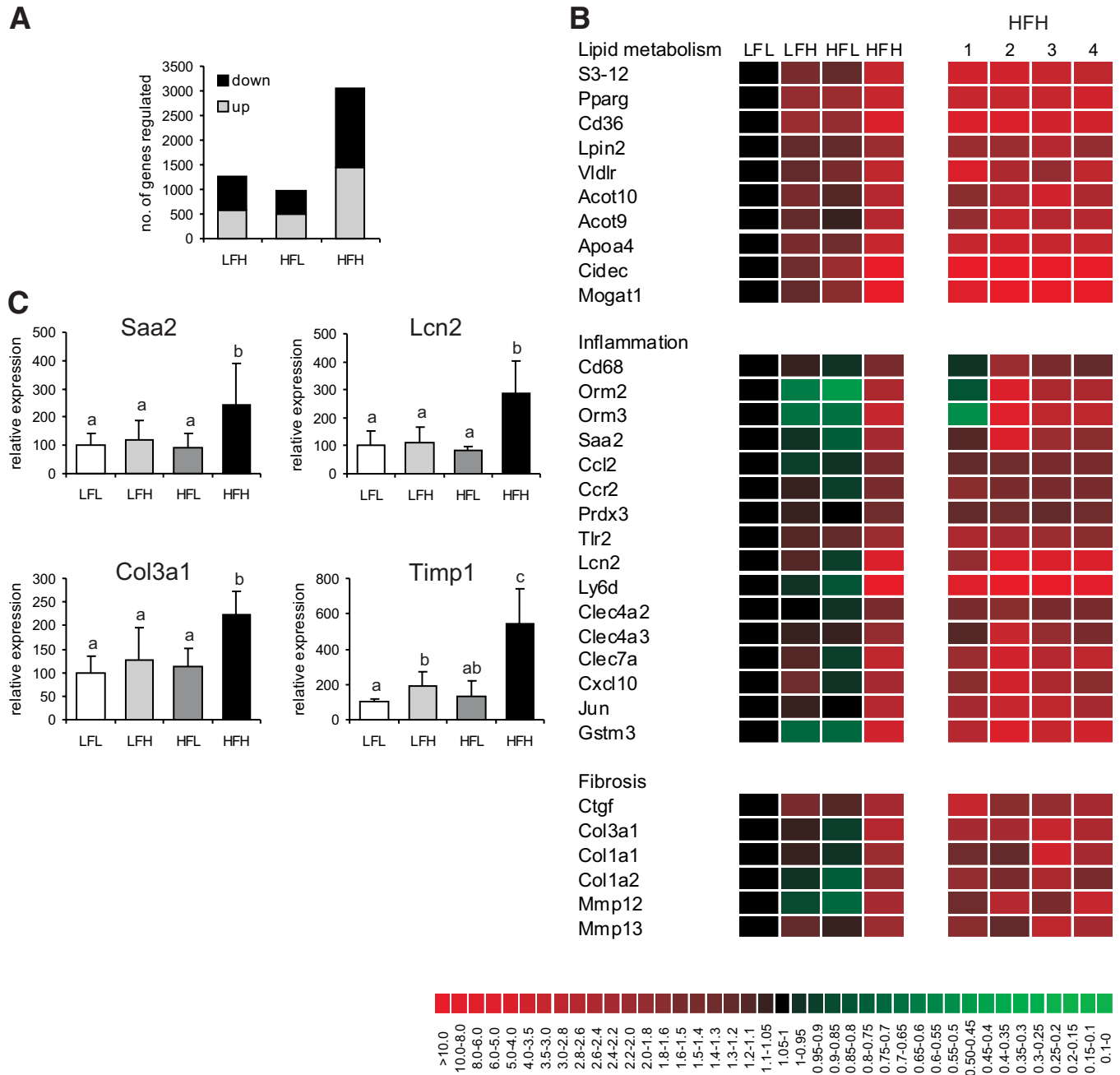
FIG. 2. Upregulation of inflammatory and fibrotic gene expression in HFH responder mice. *A*: Number of genes up- or downregulated in the various subgroups in comparison with the LFL mice as determined by Affymetrix GeneChip analysis. Genes with a *P* value <0.05 were considered significantly regulated. *B*: Heat map showing changes in expression of selected genes involved in lipid metabolism, inflammation, and fibrosis in liver. Mean expression in LFL mice was set at 1. Gene expression changes in individual mice within the HFH group are shown on the right. *C*: Changes in gene expression of selected genes as determined by real-time quantitative PCR. Mean expression in LFL mice was set at 100%. Error bars reflect SD. Bars with different letters are statistically different (*P* < 0.05 according to Student's *t* test). Number of mice per group: *n* = 4 for the LFL, HFL, and HFH groups and *n* = 6 for the LFH group.

marked and specific induction of acute phase genes encoding orosomucoid, serum amyloid-A, and lipocalin-2 in the HFH subgroup (Fig. 2*B*), and confirmed by quantitative PCR (Fig. 2*C*). Finally, many genes in the HFH expression signature were related to fibrosis, including *Ctgf*, collagens, metalloproteases, and *Timp1* (Fig. 2*B* and *C*). Expression analysis of individual mice within the HFH group showed uniform induction of genes involved in the above-mentioned pathways (Fig. 2*B*). Gene set enrichment analysis indicated that while pathways related to lipid metabolism were upregulated in all subgroups when compared with LFL mice, with most

prominent effects observed in HFH mice, numerous pathways of inflammation, cell cycle, and oxidative stress were specifically induced in HFH mice (supplemental Table 1, available in an online appendix [available at http://diabetes.diabetesjournals.org/cgi/content/full/db10-0224/DC1]). The complete microarray dataset is available at http://humannutrition2.wur.nl/duval2010.

The elevated inflammatory status in HFH livers was corroborated by immunostaining for macrophage marker Cd68 (Fig. 3*A*). Early fibrosis was detected in one HFH mouse (Fig. 3*B*). Finally, hepatic stellate activation was demonstrated in HFH mice by GFAP
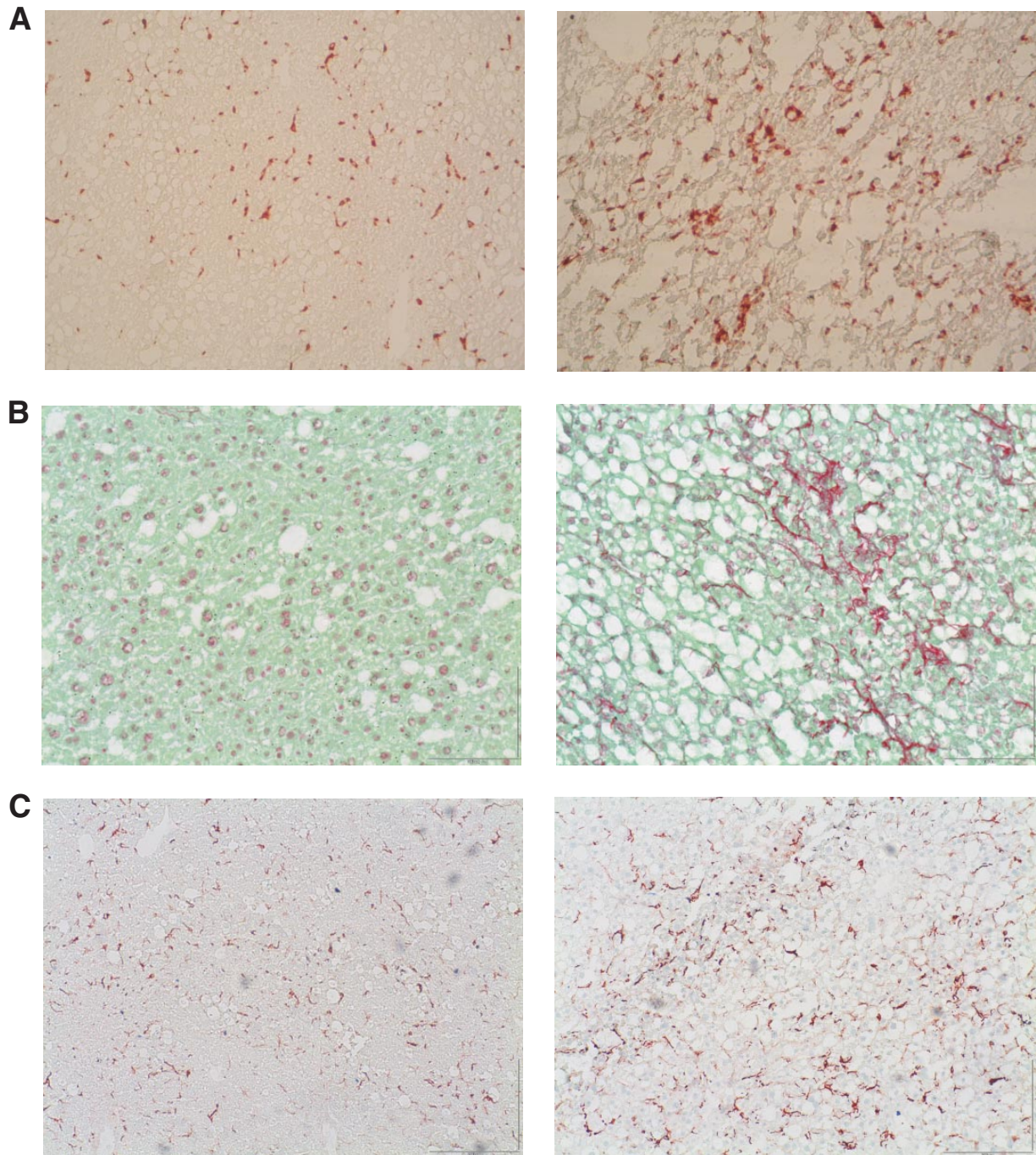
FIG. 3. (Immuno)histochemical staining confirms enhanced inflammation and early fibrosis in HFH mice. *A*: Immunohistochemical staining of macrophage activation in representative liver sections of HFL (*left panel*) and HFH (*right panel*) mice using antibody against the specific macrophage marker Cd68. *B*: Collagen staining using fast green FCF/sirius red F3B. *C*: Staining of stellate cell activation using antibody against GFAP. (A high-quality digital representation of this figure is available in the online issue.)

immunostaining (Fig. 3*C*). Overall, these analyses support induction of inflammation and fibrosis in HFH responders, indicating NASH.

HFH responder mice exhibit adipose tissue dysfunction. Mice classified as high responders also gained the most body weight (Fig. 4*A*), likely related to increased food intake (Fig. 4*B*). Indeed, a positive correlation was found between final body weight and hepatic triglycerides (Fig. 4*C*). Remarkably, despite increased weight gain, weight of the epididymal fat pad at sacrifice was markedly lower in HFH compared with that in HFL mice (Fig. 4*D*). As expected, leptin expression in adipose tissue mirrored

adiposity (Fig. 4*E*), which was also true for the plasma free fatty acids (Fig. 4*F*). Evaluation of the morphology of the epididymal fat pad in HFH mice after H-E staining revealed atrophied adipocytes surrounded by inflammatory cells, which were hardly observed in HFL responders (Fig. 4*G*). Cd68 immunostaining indicated increased presence of macrophages in HFH mice (Fig. 4*H*), which was supported by gene expression of *F4/80* and *Cd68* (Fig. 5). In contrast, expression of the anti-inflammatory adipokine adiponectin was markedly reduced in HFH mice, as was resistin (Fig. 5). Interestingly, expression of adipogenic (*Pparγ* and *Fabp4*) and lipogenic (*Dgat2*, *Srebp-1*, and fatty acid
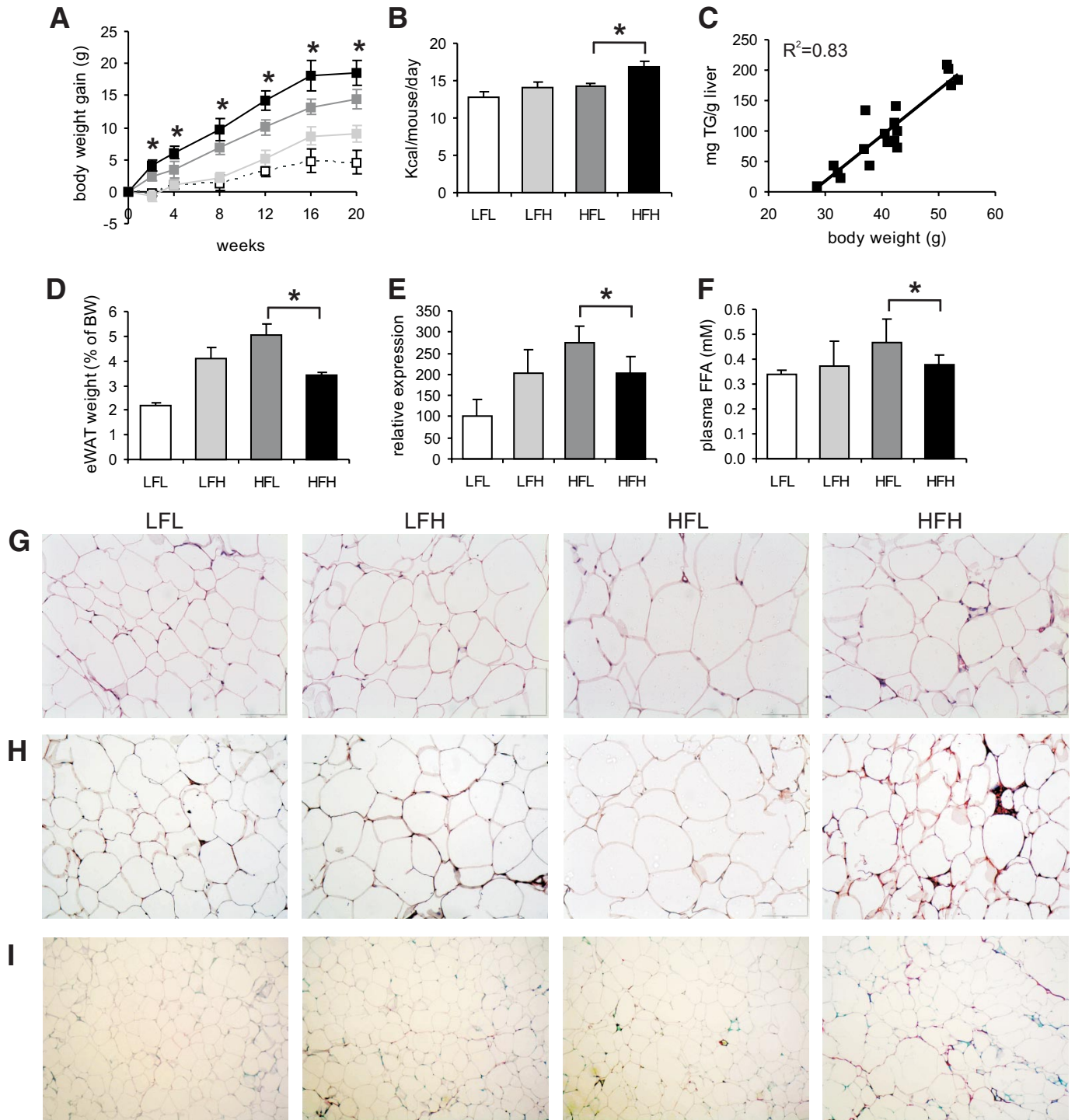
FIG. 4. Adipose dysfunction in HFH mice. *A*: Body weight changes in the four subgroups during the 21-week dietary intervention. White squares, LFL; light-gray squares, LFH; dark-gray squares, HFL; black squares, HFH. *B*: Mean daily energy intake. *C*: Positive correlation between final body weight and liver triglyceride concentration ($P < 0.05$). *D*: Weight of epididymal fat depot. *E*: Adipose tissue leptin mRNA expression as determined by quantitative PCR. Mean expression in LFL mice was set at 100%. *F*: Plasma free fatty acid levels. Error bars reflect SD. *Significantly different from HFL mice according to Student's *t* test ($P < 0.05$). Number of mice per group: $n = 4$ for LFL, HFL, and HFH and $n = 6$ for LFH. *G*: H-E staining of representative adipose tissue sections. *H*: Immunohistochemical staining of macrophages using antibody against Cd68. *I*: Collagen staining using fast green FCF/sirius red F3B. (A high-quality digital representation of this figure is available in the online issue.)

synthase, *Fasn*) marker genes was significantly downregulated in HFH mice compared with HFL mice, suggesting adipose tissue dysfunction. Finally, collagen staining revealed fibrotic adipose tissue in HFH mice (Fig. 4*I*), which was supported by increased expression of tissue inhibitor of matrix metalloproteinases (*Timp-1*) (Fig. 5). These data suggest that HFH responders, classification of which is

entirely determined by liver histology, exhibit adipose tissue dysfunction characterized by decreased fat mass, enhanced macrophage infiltration, inflammation, and adipose tissue remodelling.

Plasma biomarkers are significantly associated with liver triglycerides. To find early biomarkers that may predict NASH in C57Bl/6 mice and that may serve as
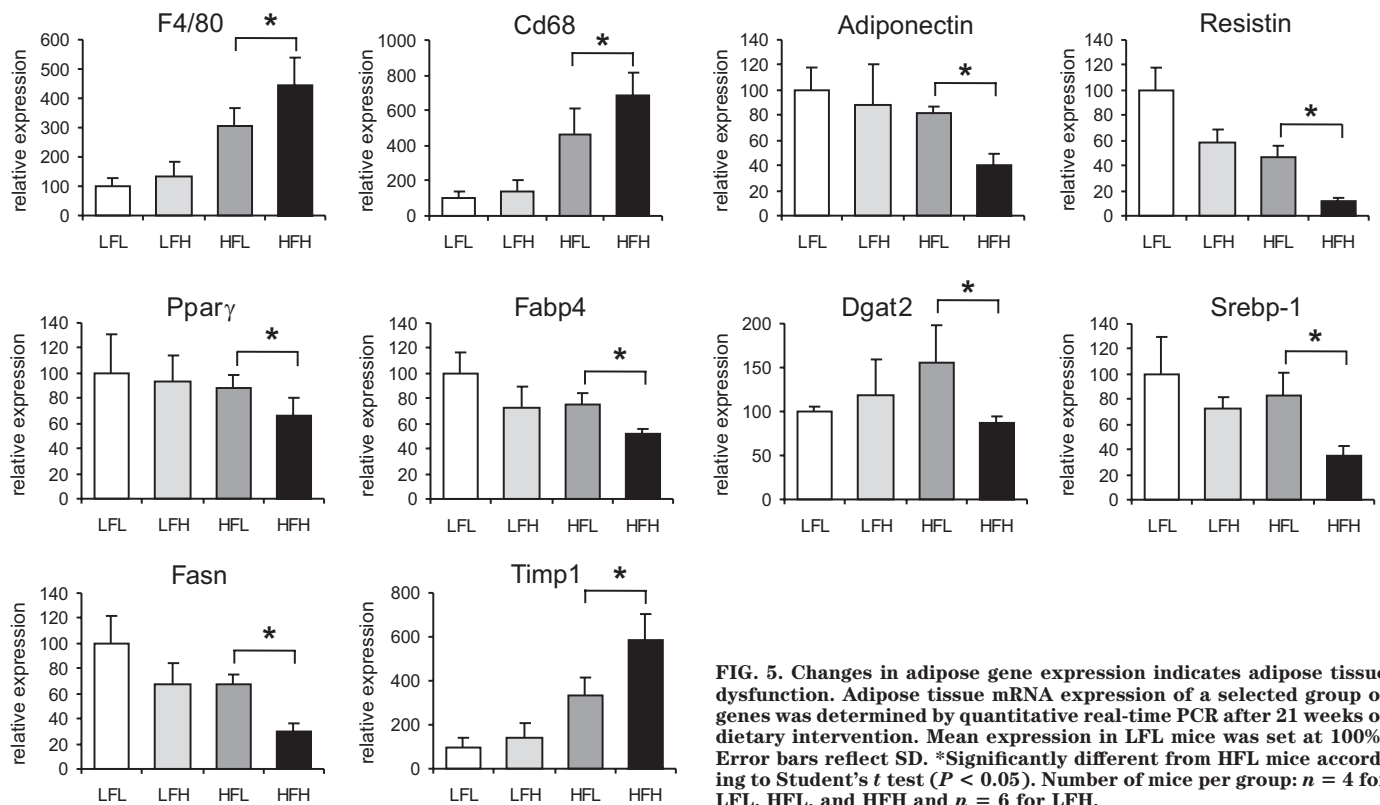
FIG. 5. Changes in adipose gene expression indicates adipose tissue dysfunction. Adipose tissue mRNA expression of a selected group of genes was determined by quantitative real-time PCR after 21 weeks of dietary intervention. Mean expression in LFL mice was set at 100%. Error bars reflect SD. *Significantly different from HFL mice according to Student's t test ($P < 0.05$). Number of mice per group: $n = 4$ for LFL, HFL, and HFH and $n = 6$ for LFH.

potential mediators between adipose tissue dysfunction and NASH, plasma was collected at different time points of diet intervention and assayed for 70 plasma proteins using multiplex analysis. Levels of most plasma proteins were not consistently different between the subgroups. One exception was the acute phase protein haptoglobin, which was elevated in HFH mice after 12 weeks of diet intervention (Fig. 6A). Similarly, plasma levels of the fibrosis marker TIMP-1 started to deviate at week 12 and further increased until the end. Remarkably, interleukin (IL)-1β and leptin levels were already elevated in HFH after 2 weeks and this pattern was maintained throughout the intervention. Finally, plasma insulin levels indicated that HFH mice became hyperinsulinemic from week 12, suggesting development of insulin resistance.

To systematically screen for plasma biomarkers that predict liver triglycerides, multivariate analysis was performed using MPLS. The results of multivariate analysis between plasma proteins at different time points and liver triglycerides are depicted in Fig. 6B and supplemental Table 2. In addition to leptin, plasma levels of C-reactive protein (CRP), eotaxin, haptoglobin, and macrophage inflammatory protein (MIP)-1α early in the intervention were positively associated with liver triglycerides at 20 weeks. Intermediate prognostic markers of liver triglycerides included IL-18, IL-1β, MIP-1γ, and MIP-2, whereas insulin, TIMP-1, GCP-2, and MPO emerged as late markers. Throughout the diet intervention, highest regression coefficients were obtained for CRP, haptoglobin, leptin, and IL-1β (supplemental Table 2). Adiponectin was not significantly associated with liver triglycerides. The complete multivariate dataset is available at http://humannutrition2.wur.nl/duval2010. Besides potentially serving as predictive biomarkers of liver triglycerides, these proteins may provide a functional link between adipose tissue dysfunction and NAFLD.

DISCUSSION

C57Bl/6 mice fed a HFD represent a popular animal model for human obesity and insulin resistance. Despite development of hepatic steatosis and other features of patients with NAFLD (18), except for a recent report the model has not been extensively used to study NAFLD (19). As expected, high-fat feeding increased adipose tissue mass and hepatic fat storage. Consistent with previous data showing considerable variability in the obese and diabetic phenotype (20,21), we observed marked heterogeneity in body weight gain. Additionally, the magnitude of fat storage and NAFLD scoring differed markedly between the mice, giving rise to four well-distinguishable groups. Detailed histological and gene expression analysis indicated that HFH mice exhibit NASH. Accordingly, detailed study of these HFH responders may give novel insight into the development and progression of NAFLD.

Although humans have no epididymal fat pads, we studied epididymal adipose tissue because it represents the most commonly used fat depot in mouse studies, is easily accessible, can be accurately weighed, and is relatively homogenous. Unfortunately, we did not have access to dual-energy X-ray absorptiometry or magnetic resonance imaging to be able to measure fat percentage, lean body mass, or fat distribution. Remarkably, HFH mice, despite showing the highest weight gain, had significantly less epididymal fat after 21 weeks compared with HFL mice, which likely reflects differences in overall adiposity. An important question is why there is an apparent limit to the expansion of adipose tissue in HFH mice and, especially, what is the link with NASH. Obesity-related adipocyte hypertrophy is known to be associated with adipose inflammation characterized by infiltration of macrophages and other leukocytes, appearance of so-called crown-like structures, and increased expression of several inflamma-
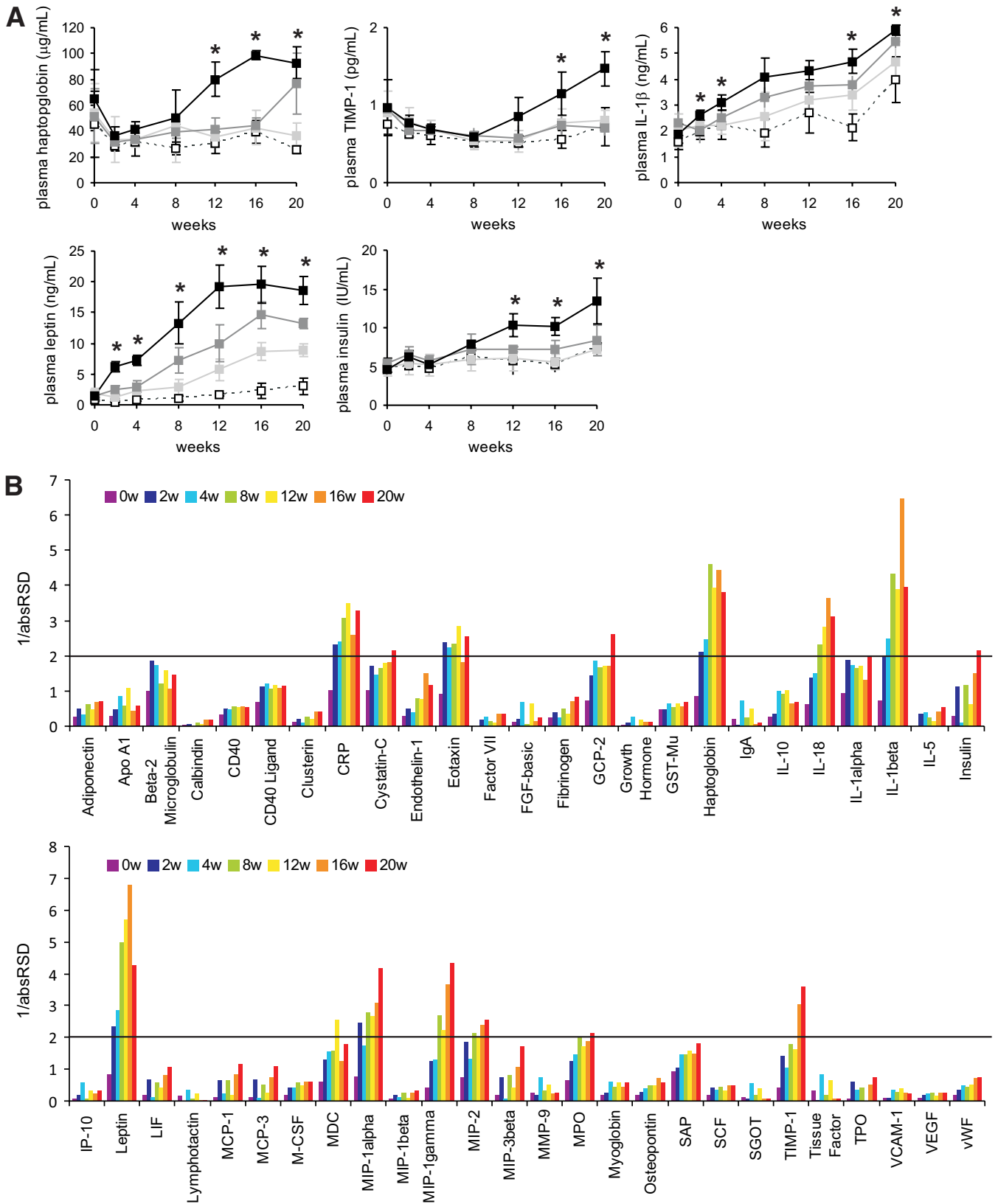
FIG. 6. Plasma proteins as early predictive biomarker for NASH in C57Bl/6 mice. *A*: Plasma concentration of haptoglobin, TIMP-1, IL-1β, leptin, and insulin were determined by multiplex assay at specific time points during the 21 weeks of dietary intervention after a 6-h fast. White squares, LFL; light-gray squares, LFH; dark-gray squares, HFL; black squares, HFH. Error bars reflect SD. *Significantly different from HFL mice according to Student's *t* test ($P < 0.05$). Number of mice per group: $n = 4$ for LFL, HFL, and HFH and $n = 6$ for LFH. *B*: Graphs illustrating the result of multivariate analysis showing the association of protein plasma concentrations at various time points with final liver triglyceride content. The absRSD is the absolute relative standard deviation: the standard deviation of the regression coefficients divided by the absolute mean value of the regression coefficients. Significant proteins display an inverse absRSD value higher than two (bold line indicates the inverse absRSD threshold value of 2). w, weeks.

tory markers (2,3,22,23). How adipose tissue inflammation develops during obesity is not clear, but a role of hypertrophy, hypoxia, and adipocyte cell death has been suggested (23,24). Compared with HFL mice, adipose tissue of HFH mice showed more pronounced inflammation as shown by increased macrophage staining and expression of inflammatory marker genes and increased collagen staining, suggesting fibrosis. Furthermore, decreased adipocyte size and increased cell death were observed in HFH mice. Since HFH mice are classified entirely based on liver histology, these data indicate a strong link between inflammatory and morphological changes in adipose tissue and progression of steatosis to NASH. Consequently, adipose tissue failure or dysfunction may signal progression of hepatic steatosis toward NASH. These data support the previous suggestion that poor expansion of adipose tissue mass due to remodeling contributes to hepatic steatosis induced by high-fat feeding (23) and thereby strengthen an emerging view that obesity starts to cause metabolic problems when adipose tissue cannot fully meet demands for additional storage, leading to fat accumulation in other organs such as muscle, liver, and β-cells and causing lipotoxicity (25–27). The limited expandability of adipose tissue may be related to adipose tissue fibrosis and associated disproportionate accumulation of extracellular matrix components (22).

Multivariate longitudinal analysis of plasma proteins yielded a number of candidates that may serve as prognostic markers for NAFLD and NASH. In addition, these proteins may provide insight into the functional link between adipose tissue dysfunction and NAFLD. Besides leptin, the best predictive markers were the acute phase proteins CRP and haptoglobin and MIP-1α (Ccl3). Plasma CRP was previously proposed as a diagnostic marker for NASH (28). In one study, high-sensitivity CRP was significantly elevated in patients with NASH compared with that in patients with only steatosis (29). Furthermore, high-sensitivity CRP correlated with the severity of fibrosis in NASH. In another study, plasma CRP was not helpful in diagnosis of NASH in severely obese patients, possibly because adipose tissue contributes to plasma CRP in obesity.

Hardly any data exist on the relation between plasma haptoglobin and NASH. Haptoglobin was included in a composite biomarker combining 13 parameters to predict NASH (30). Interestingly, in a recent study plasma haptoglobin showed a negative correlation with fibrosis stage (31). There are no reports on the association between plasma MIP-1α and hepatic steatosis or NASH. However, it was reported that MIP-1α mRNA in human liver is positively associated with liver fat (32).

Another good predictive marker for liver triglycerides was IL-1β. Plasma IL-1β levels were significantly elevated in HFH mice already after 2 weeks of HFD, probably because of elevated production in adipose tissue. Recently, we showed that IL-1β may promote steatosis in mice by inhibiting PPARα activity (33). Whether adipose tissue–derived IL-1β links adipose tissue dysfunction and NASH requires further study.

Recent studies indicate that IL-18 promotes hepatic steatosis in mice (34,35). Interestingly, patients with NAFLD were found to have significantly elevated plasma IL-18 levels (36). According to our multivariate analysis, plasma IL-18 from week eight onward was significantly associated with liver triglycerides. Overall, further research into the potential use of plasma CRP, haptoglobin,

MIP-1α, and possibly IL-1β, eotaxin, and IL-18 as prognostic biomarkers for NAFLD in humans is warranted.

One of the late biomarkers to emerge from our study was TIMP-1. Specifically, plasma TIMP-1 levels started to deviate in the HFH mice after 12 weeks of HFD. Since TIMP-1 expression was increased in HFH mice in both liver and adipose tissue, it is unclear which tissue primarily contributes to increased plasma levels. TIMP-1 is used extensively as a marker of fibrosis related to viral hepatitis (37). However, its use in the context of NAFLD is very limited. According to our data, plasma TIMP-1 levels may have potential as a biomarker for NASH. Consistent with this notion, plasma TIMP-1 was recently shown to be a valuable component of a composite predictive marker of NASH in human (38).

An adipokine that has been extensively linked to NAFLD is adiponectin (37,39). Besides its antisteatotic role (38,40), adiponectin has potent anti-inflammatory effects in liver (39). In humans, plasma adiponectin, either alone or as ratio to plasma leptin (41), has shown promise as a diagnostic marker for NASH, although it should be validated in larger cohorts of patients (9). In the present study, plasma adiponectin was not significantly associated with liver triglycerides.

Overall, the best predictive marker for liver triglycerides, which was also clearly elevated in HFH mice, was leptin. Portal infusion with leptin was shown to increase hepatic triglycerides in rats (42). Furthermore, leptin appears to be one of the key regulators of inflammation and progression to fibrosis in NASH (43–46). Although some studies have found elevated plasma leptin levels in patients with NASH (47,48), other studies have not, thus somewhat questioning the potential of plasma leptin as a noninvasive marker for diagnosis of NASH in humans (49).

Hyperleptinemia in HFH mice is expected to decrease food intake. However, energy intake was higher in HFH compared with that in other subgroups, suggesting existence of leptin resistance, at least centrally in the hypothalamus. In contrast, leptin resistance is expected to be absent from liver, in which chronically elevated leptin levels may promote NASH by stimulating hepatic triglyceride storage, inflammation, and fibrosis (37). Leptin resistance may thus be the basis for hyperleptinemia and hyperphagia in HFH mice, leading to accelerated weight and fat gain and consequent adipose tissue dysfunction.

The significant heterogeneity in the response to HFD in C57Bl/6 mice has been previously reported (20,21). The underlying reason for the large heterogeneity is uncertain but may be related to copy no. variations in the mouse genome (50) and perhaps specifically by differences in the copy no. of the *Ide* gene encoding the insulin-degrading enzyme (51). Alternatively, the variation in phenotype after HFD may be mediated by epigenetic mechanisms (21), giving rise to variable adipose expression of specific genes. However, the importance of epigenetic mechanisms in controlling expression of one of these genes was later discounted (52). Overall, the relative importance of genetic, epigenetic, and environmental factors in the response to high-fat feeding in C57Bl/6 mice is still unclear.

In conclusion, we show that a subset of C57Bl/6 mice fed a HFD composed of palm oil developed NASH. Our data support the existence of a tight relationship between adipose tissue dysfunction and NASH pathogenesis and point to several novel potential predictive biomarkers for NASH.

ACKNOWLEDGMENTS

REFERENCES

1. Perlemuter G, Bigorgne A, Cassard-Doulcier AM, Naveau S. Nonalcoholic fatty liver disease: from pathogenesis to patient care. Nat Clin Pract Endocrinol Metab 2007;3:458–469
2. Weisberg SP, McCann D, Desai M, Rosenbaum M, Leibel RL, Ferrante AW Jr.: Obesity is associated with macrophage accumulation in adipose tissue. J Clin Invest 2003;112:1796–1808
3. Xu H, Barnes GT, Yang Q, Tan G, Yang D, Chou CJ, Sole J, Nichols A, Ross JS, Tartaglia LA, Chen H. Chronic inflammation in fat plays a crucial role in the development of obesity-related insulin resistance. J Clin Invest 2003;112:1821–1830
4. Lazar MA. How obesity causes diabetes: not a tall tale. Science 2005;307: 373–375
5. Szendroedi J, Roden M. Ectopic lipids and organ function. Curr Opin Lipidol 2009;20:50–56
6. Yeh MM, Brunt EM. Pathology of nonalcoholic fatty liver disease. Am J Clin Pathol 2007;128:837–847
7. Lalor PF, Faint J, Aarbodem Y, Hubscher SG, Adams DH. The role of cytokines and chemokines in the development of steatohepatitis. Semin Liver Dis 2007;27:173–193
8. Jou J, Choi SS, Diehl AM. Mechanisms of disease progression in nonalcoholic fatty liver disease. Semin Liver Dis 2008;28:370–379
9. Tsochatzis EA, Papatheodoridis GV, Archimandritis AJ. Adipokines in nonalcoholic steatohepatitis: from pathogenesis to implications in diagnosis and therapy. Mediators Inflamm 2009;831670
10. Stienstra R, Mandard S, Patsouris D, Maass C, Kersten S, Muller M. Peroxisome proliferator-activated receptor alpha protects against obesity-induced hepatic inflammations. Endocrinology 2007;148:2753–2763
11. Rakhshandehroo M, Hooiveld G, Muller M, Kersten S. Comparative analysis of gene regulation by the transcription factor PPARalpha between mouse and human. PLoS One 2009;4:e6796
12. Sanderson LM, Degenhardt T, Koppen A, Kalkhoven E, Desvergne B, Muller M, Kersten S. Peroxisome proliferator-activated receptor beta/delta (PPARbeta/delta) but not PPARalpha serves as a plasma free fatty acid sensor in liver. Mol Cell Biol 2009;29:6257–6267
13. Subramanian A, Tamayo P, Mootha VK, Mukherjee S, Ebert BL, Gillette MA, Paulovich A, Pomeroy SL, Golub TR, Lander ES, Mesirov JP. Gene set enrichment analysis: a knowledge-based approach for interpreting genome-wide expression profiles. Proc Natl Acad Sci U S A 2005;102:15545–15550
14. Boulesteix AL, Strimmer K. Partial least squares: a versatile tool for the analysis of high-dimensional genomic data. Brief Bioinform 2007;8:32–44
15. Bro R. Multiway calibration multilinear PLS. J Chemometrics 1996;10: 47–62
16. Smilde AK, Bro R, Geladi P. *Multi-Way Analysis: Applications in the Chemical Sciences.* West Sussex, Wiley, 2004
17. Heidema AG, Thissen U, Boer JM, Bouwman FG, Feskens EJ, Mariman EC. The association of 83 plasma proteins with CHD mortality, BMI, HDL-, and total-cholesterol in men: applying multivariate statistics to identify proteins with prognostic value and biological relevance. J Proteome Res 2009;8:2640–2649
18. Larter CZ, Yeh MM. Animal models of NASH: getting both pathology and metabolic context right. J Gastroenterol Hepatol 2008;23:1635–1648
19. Ito M, Suzuki J, Tsujioka S, Sasaki M, Gomori A, Shirakura T, Hirose H, Ishihara A, Iwaasa H, Kanatani A. Longitudinal analysis of murine steato-hepatitis model induced by chronic exposure to high-fat diet. Hepatol Res 2007;37:50–57
20. Burcelin R, Crivelli V, Dacosta A, Roy-Tirelli A, Thorens B. Heterogeneous metabolic adaptation of C57BL/6J mice to high-fat diet. Am J Physiol Endocrinol Metab 2002;282:E834–E842
21. Koza RA, Nikonova L, Hogan J, Rim JS, Mendoza T, Faulk C, Skaf J, Kozak LP. Changes in gene expression foreshadow diet-induced obesity in genetically identical mice. PLoS Genet 2006;2:e81
22. Khan T, Muise ES, Iyengar P, Wang ZV, Chandalia M, Abate N, Zhang BB, Bonaldo P, Chua S, Scherer PE. Metabolic dysregulation and adipose tissue fibrosis: role of collagen VI. Mol Cell Biol 2009;29:1575–1591
23. Strissel KJ, Stancheva Z, Miyoshi H, Perfield JW 2nd, DeFuria J, Jick Z, Greenberg AS, Obin MS. Adipocyte death, adipose tissue remodeling, and obesity complications. Diabetes 2007;56:2910–2918
24. Trayhurn P, Wang B, Wood IS. Hypoxia in adipose tissue: a basis for the dysregulation of tissue function in obesity? Br J Nutr 2008;100:227–235
25. Tan CY, Vidal-Puig A. Adipose tissue expandability: the metabolic problems of obesity may arise from the inability to become more obese. Biochem Soc Trans 2008;36:935–940
26. Unger RH. The physiology of cellular liporegulation. Annu Rev Physiol 2003;65:333–347
27. Wang MY, Grayburn P, Chen S, Ravazzola M, Orci L, Unger RH. Adipogenic capacity and the susceptibility to type 2 diabetes and metabolic syndrome. Proc Natl Acad Sci U S A 2008;105:6139–6144
28. Uchihara M, Izumi N. [High-sensitivity C-reactive protein (hs-CRP): a promising biomarker for the screening of non-alcoholic steatohepatitis (NASH)]. Nippon Rinsho 2006;64:1133–1138 [in Japanese]
29. Yoneda M, Mawatari H, Fujita K, Iida H, Yonemitsu K, Kato S, Takahashi H, Kirikoshi H, Inamori M, Nozaki Y, Abe Y, Kubota K, Saito S, Iwasaki T, Terauchi Y, Togo S, Maeyama S, Nakajima A. High-sensitivity C-reactive protein is an independent clinical feature of nonalcoholic steatohepatitis (NASH) and also of the severity of fibrosis in NASH. J Gastroenterol 2007;42:573–582
30. Poynard T, Ratziu V, Charlotte F, Messous D, Munteanu M, Imbert-Bismut F, Massard J, Bonyhay L, Tahiri M, Thabut D, Cadranel JF, Le Bail B, de Ledinghen V. Diagnostic value of biochemical markers (NashTest) for the prediction of non alcoholo steato hepatitis in patients with non-alcoholic fatty liver disease. BMC Gastroenterol 2006;6:34
31. Lee HH, Seo YS, Um SH, Won NH, Yoo H, Jung ES, Kwon YD, Park S, Keum B, Kim YS, Yim HJ, Jeen YT, Chun HJ, Kim CD, Ryu HS. Usefulness of non-invasive markers for predicting significant fibrosis in patients with chronic liver disease. J Korean Med Sci 2010;25:67–74
32. Westerbacka J, Kolak M, Kiviluoto T, Arkkila P, Siren J, Hamsten A, Fisher RM, Yki-Jarvinen H. Genes involved in fatty acid partitioning and binding, lipolysis, monocyte/macrophage recruitment, and inflammation are over-expressed in the human fatty liver of insulin-resistant subjects. Diabetes 2007;56:2759–2765
33. Stienstra R, Saudale F, Duval C, Keshtkar S, Groener JE, van Rooijen N, Staels B, Kersten S, Muller M: Kupffer cells promote hepatic steatosis via interleukin-1beta-dependent suppression of peroxisome proliferator-activated receptor alpha activity. Hepatology 51:511–522
34. Chikano S, Sawada K, Shimoyama T, Kashiwamura SI, Sugihara A, Sekikawa K, Terada N, Nakanishi K, Okamura H. IL-18 and IL-12 induce intestinal inflammation and fatty liver in mice in an IFN-gamma dependent manner. Gut 2000;47:779–786
35. Kaneda M, Kashiwamura S, Ueda H, Sawada K, Sugihara A, Terada N, Kimura-Shimmyo A, Fukuda Y, Shimoyama T, Okamura H. Inflammatory liver steatosis caused by IL-12 and IL-18. J Interferon Cytokine Res 2003;23:155–162
36. Li Y, Li-Li Z, Qin L, Ying W. Plasma interleukin-18/interleukin-18 binding protein ratio in Chinese with NAFLD. Hepatogastroenterology 2010;57: 103–106
37. Schaffler A, Scholmerich J, Buchler C. Mechanisms of disease: adipocytokines and visceral adipose tissue–emerging role in nonalcoholic fatty liver disease. Nat Clin Pract Gastroenterol Hepatol 2005;2:273–280
38. Xu A, Wang Y, Keshaw H, Xu LY, Lam KS, Cooper GJ. The fat-derived hormone adiponectin alleviates alcoholic and nonalcoholic fatty liver diseases in mice. J Clin Invest 2003;112:91–100
39. Marra F, Bertolani C. Adipokines in liver diseases. Hepatology 2009;50: 957–969
40. Yamauchi T, Kamon J, Waki H, Terauchi Y, Kubota N, Hara K, Mori Y, Ide T, Murakami K, Tsuboyama-Kasaoka N, Ezaki O, Akanuma Y, Gavrilova O, Vinson C, Reitman ML, Kagechika H, Shudo K, Yoda M, Nakano Y, Tobe K, Nagai R, Kimura S, Tomita M, Froguel P, Kadowaki T. The fat-derived hormone adiponectin reverses insulin resistance associated with both lipoatrophy and obesity. Nat Med 2001;7:941–946
41. Lemoine M, Ratziu V, Kim M, Maachi M, Wendum D, Paye F, Bastard JP,

Poupon R, Housset C, Capeau J, Serfaty L. Serum adipokine levels predictive of liver injury in non-alcoholic fatty liver disease. Liver Int 2009;29:1431–1438

42. Roden M, Anderwald C, Furnsinn C, Waldhausl W, Lohninger A. Effects of short-term leptin exposure on triglyceride deposition in rat liver. Hepatology 2000;32:1045–1049

43. Ikejima K, Honda H, Yoshikawa M, Hirose M, Kitamura T, Takei Y, Sato N. Leptin augments inflammatory and profibrogenic responses in the murine liver induced by hepatotoxic chemicals. Hepatology 2001;34:288–297

44. Ikejima K, Okumura K, Lang T, Honda H, Abe W, Yamashina S, Enomoto N, Takei Y, Sato N. The role of leptin in progression of non-alcoholic fatty liver disease. Hepatol Res 2005;33:151–154

45. Leclercq IA, Farrell GC, Schriemer R, Robertson GR. Leptin is essential for the hepatic fibrogenic response to chronic liver injury. J Hepatol 2002;37:206–213

46. Saxena NK, Ikeda K, Rockey DC, Friedman SL, Anania FA. Leptin in hepatic fibrosis: evidence for increased collagen production in stellate cells and lean littermates of ob/ob mice. Hepatology 2002;35:762–771

47. Chitturi S, Farrell G, Frost L, Kriketos A, Lin R, Fung C, Liddle C, Samarasinghe D, George J. Serum leptin in NASH correlates with hepatic steatosis but not fibrosis: a manifestation of lipotoxicity? Hepatology 2002;36:403–409

48. Krawczyk K, Szczesniak P, Kumor A, Jasinska A, Omulecka A, Pietruczuk M, Orszulak-Michalak D, Sporny S, Malecka-Panas E. Adipohormones as prognostric markers in patients with nonalcoholic steatohepatitis (NASH). J Physiol Pharmacol 2009;60(Suppl. 3):71–75

49. Tsochatzis E, Papatheodoridis GV, Archimandritis AJ. The evolving role of leptin and adiponectin in chronic liver diseases. Am J Gastroenterol 2006;101:2629–2640

50. Cutler G, Kassner PD. Copy number variation in the mouse genome: implications for the mouse as a model organism for human disease. Cytogenet Genome Res 2008;123:297–306

51. Watkins-Chow DE, Pavan WJ. Genomic copy number and expression variation within the C57BL/6J inbred mouse strain. Genome Res 2008;18:60–66

52. Koza RA, Rogers P, Kozak LP. Inter-individual variation of dietary fat-induced mesoderm specific transcript in adipose tissue within inbred mice is not caused by altered promoter methylation. Epigenetics 2009;4:512–518